

Estimation of Scatterer Diameter Using Ultrasonic Backscattering Property for Assessment of Red Blood Cell Aggregation

Nobutaka Saitoh¹, Hideyuki Hasegawa^{2,1}, and Hiroshi Kanai^{1,2,*}

¹Graduate School of Engineering, Tohoku University, Sendai 980-8579, Japan

²Graduate School of Biomedical Engineering, Tohoku University, Sendai 980-8579, Japan

Received November 19, 2008; accepted April 5, 2009; published online July 21, 2009

Red blood cell (RBC) aggregation, a determinant of blood viscosity, plays an important role in blood flow rheology. RBC aggregation is induced by the adhesion of RBCs when the electrostatic repulsion between RBCs weakens owing to increases in protein and saturated fatty acid levels in blood, and excessive RBC aggregation may lead to various circulatory diseases. This study was conducted to establish a noninvasive quantitative method for the assessment of RBC aggregation. The spectrum of nonaggregating RBCs presents Rayleigh behavior, indicating that the power of a scattered wave is proportional to the fourth power of frequency. By dividing the measured power spectrum of echoes from scatterers by that from a silicone plate reflector, the frequency responses of transmitting and receiving transducers are removed from the former spectrum. This normalized power spectrum changes linearly with respect to logarithmic frequency. In non-Rayleigh scattering, on the other hand, the spectral slope decreases because a larger scatterer behaves as a reflector and echoes from a reflector do not show frequency dependence. Therefore, it is possible to assess RBC aggregation using the spectral slope value. In this study, spherical scatterers with diameters of 5, 11, 15, and 30 μm were measured in basic experiments. The spectral slope of the normalized power spectrum of echoes from the lumen of the vein in the dorsum manus of a 24-year-old healthy male was close to that from microspheres with a diameter of 15 μm , and the typical RBC diameter was smaller than this value. The frequency-dependent attenuation of ultrasound during propagation in a biomedical tissue was considered to be one reason for this. Furthermore, during avascularization, the slope gradually decreased owing to the aggregation of RBCs. These results show the possibility of using the proposed method for the noninvasive assessment of RBC aggregation. © 2009 The Japan Society of Applied Physics

DOI: 10.1143/JJAP.48.07GJ08

1. Introduction

Medical ultrasound is clinically used to make a diagnosis for various organs, and because it is noninvasive and relatively stress free for patients, it can be repeatedly employed to confirm time-dependent changes. Ultrasound B-mode imaging is widely used for the morphological diagnosis of the arterial wall. In addition, methods for evaluating the viscoelasticity of the arterial wall have recently been developed^{1,2)} because the mechanical properties of the arterial wall are related to the atherosclerotic change.

The condition of blood is an important factor related to various circulatory diseases. However, conventional ultrasonic images cannot be used to evaluate the condition of the blood in the blood vessel because red blood cells (RBCs), which are the main components of blood, are much smaller than the wavelength of ultrasound and the variation in acoustic impedance between blood plasma and RBCs is very small. However, the condition of blood is related to various circulatory diseases, and the evaluation and diagnosis of such a condition are important for the detection of a disease at an early stage.

As one of the determinants of blood viscosity, RBC aggregation plays an important role in blood flow rheology. The adventitia of healthy RBCs is charged with negative electricity, which impedes RBC adherence by electrostatic repulsion.³⁾ However, owing to increases in protein and saturated fatty acid levels in blood, such repulsion between RBCs is gradually weakened and RBC aggregation is induced by the overlapping of RBCs. The main function of blood is to transport nutrients, oxygen, and essential elements to tissues and to remove metabolic products, such as carbon dioxide and lactic acid, produced by those tissues.⁴⁾ However, RBC aggregation significantly degrades this function because of the decrease in the superficial area

used to transport materials. Excessive RBC aggregation may promote various circulatory diseases, such as atherosclerosis, hypercholesterolemia, diabetes, thrombosis, and so on.⁵⁻⁸⁾ Therefore, the assessment of RBC aggregation is essential.⁹⁾ The micro channel array flow analyzer (MC-FAN) method is a recently developed technique for the assessment of RBC aggregation by determining whether red blood cells pass through gaps in silicon substrates simulating blood capillaries.¹⁰⁾ However, this method is invasive and is not quantitative. The present study was conducted to establish a noninvasive quantitative method for the assessment of RBC aggregation.

2. Principles

An RBC is a very small ultrasonic scatterer whose diameter is 8 μm at most, and thus, the amplitudes of scattered RF echoes are very small. To assess the level of RBC aggregation, the power spectrum of the echoes from RBCs is calculated using the fast Fourier transform (FFT), and the scattering properties of RF echoes are evaluated in the frequency domain. In the present study, it was assumed that the diameter of a scatterer increases depending on the degree of RBC aggregation.

The scattering strength can be measured quantitatively in terms of a backscattering coefficient if the tissues can be modeled as a random medium. Figure 1 shows the geometrical condition in the measurement of echoes from a random medium with a circular transducer.¹¹⁾ The average power spectrum $S_i(f)$ of incoherent components of the echo scattered by the random medium is given by¹¹⁾

$$S_i(f) = |4\pi f \rho_0 G(f)|^2 k^4 R_s^2 g(f) \left(\frac{S_0}{2\pi w_0} \right)^4, \quad (2.1)$$

where k is the wave number of ultrasonic waves ($k = 2\pi f / c_0$, c_0 is the average sound velocity), ρ_0 is the average density of the medium, $G(f)$ is the electric characteristic of the transducer, R_s is the standard deviation of the amplitude

*E-mail address: kanai@ecei.tohoku.ac.jp

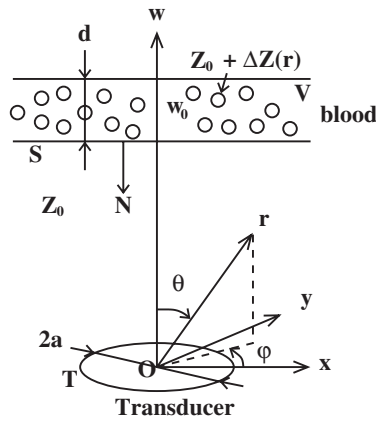


Fig. 1. Illustration of geometrical condition in measurement of echoes from scatterers with a circular transducer.

reflection coefficients of scatterers, S_0 is the area of the transducer aperture, and w_0 is the distance between the transducer and the scatterers. Furthermore, $g(f)$ is expressed as

$$g(f) = \left(\frac{\pi^{2.5} \sigma_b^2 d \sigma}{4} \right) (\sigma_b^{-2} + \sigma_T^{-2} + \sigma^{-2})^{-1} e^{-\sigma^2 k^2}, \quad (2.2)$$

where d is the thickness of the layer of the medium including scatterers, σ_b and σ_T are the beam radius ($\sigma_b = \sqrt{8}w_0/ka$) and $a/\sqrt{2}$ (a : aperture radius), respectively, and σ is the correlation length of continuous inhomogeneous media,¹²⁾ σ being related to the diameter of the scatterer.¹¹⁾ In this case, the correlation length is much smaller than the diameter and beam width of the transducer. Therefore, the following approximation holds:

$$(\sigma_b^{-2} + \sigma_T^{-2} + \sigma^{-2})^{-1} = \left\{ \sigma^{-2} \left[\left(\frac{\sigma_b}{\sigma} \right)^{-2} + \left(\frac{\sigma_T}{\sigma} \right)^{-2} + 1 \right] \right\}^{-1} \approx \sigma^2. \quad (2.3)$$

Using eq. (2.3), eq. (2.1) is modified as

$$S_i(f) = [|G(f)|^2 Z_0^2 R_s^2 d] \left(\frac{a^6}{w_0^2} \right) \left(\frac{\pi^{2.5} k^4 \sigma^3 e^{-k^2 \sigma^2}}{2} \right), \quad (2.4)$$

where Z_0 is the average specific acoustic impedance of the medium. When scatterer diameters are sufficiently smaller than the ultrasonic wavelength [$k\sigma \ll 1$, $e^{-k^2 \sigma^2} \simeq 1$, $S_i(f) \propto k^4 \sigma^6$], echoes from scatterers show Rayleigh behavior, i.e., the power $S_i(f)$ of scattered waves is proportional to the fourth power of frequency, f^4 .^{11,13,14)} Echoes from scatterers with larger diameters include the components of reflection, which have no frequency dependence. Therefore, the spectral slope decreases when the sizes of scatterers increase and the components of reflection are included in the echoes.¹⁵⁾

The measured power spectrum $P_s(f)$ of the received ultrasonic echo signal $e_s(t)$ contains both the scattering property $S_i(f)$ from a microscopic sphere and the frequency responses $G(f)$ of transmitting and receiving transducers. Therefore, by normalizing the power spectrum $P_s(f)$ of echoes from scatterers by the power spectrum $P_r(f)$ from a silicone plate, the frequency responses $G(f)$ of the transmitting and receiving transducers are removed.¹⁶⁻¹⁸⁾

Figure 2 shows a system for measuring an echo $e_r(t)$ from a silicone plate. The distance between the probe and the

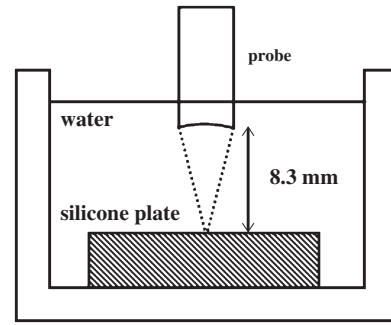


Fig. 2. System for measurement of echoes from the silicone plate.

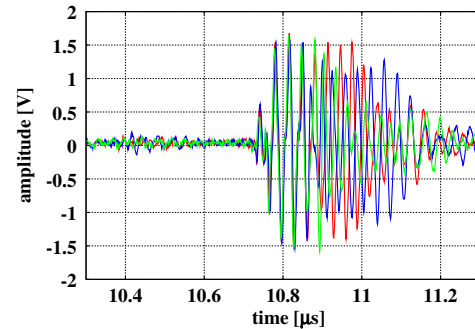


Fig. 3. (Color online) Three RF echoes from the silicone plate at different points on the surface.

silicone plate was equal to that between the probe and the middle part of the intravascular lumen in an *in vivo* measurement. Figure 3 shows RF echoes reflected by the surface of the silicone plate and scattered from the inside of the silicone plate. Three lines in Fig. 3 show RF signals from different points of the silicone plate. The scatterer distribution in the silicone plate is assumed to be random, and only the echo reflected from the surface can be obtained by averaging the echoes measured at different points on the surface. Therefore, echoes from the silicone plate were acquired at 1000 different points by moving the transducer. In Fig. 3, there are echoes with much smaller amplitudes of around 10.4 μ s. Such echoes were supposed to be caused by the interference of ultrasonic waves during focusing by the concave transducer used.¹⁹⁾ Such undesirable echoes were suppressed by applying Hanning windows centered at 10.8 μ s when the Fourier transform was performed. Figure 4 shows the power spectrum $P_r(f)$ from a silicone plate that was obtained by averaging 1000 power spectra of RF echoes from a number of different points on the surface of the silicone plate. The frequency range used for normalization was limited because the ultrasonic pulse used in this study had a finite frequency bandwidth. In the present study, we estimated the slope a of the normalized power spectrum $P_s(f)/P_r(f)$ using the weighted least-mean-squared method by considering the signal-to-noise ratio (SNR) of the echo at each frequency.²⁰⁾ Let us define the mean squared difference between the measured spectrum and a linear model as

$$\alpha = \sum_{i=0}^N e_i^2 = \sum_{i=0}^N w_i^2 [y(f_i) - (ax_i + b)]^2, \quad (2.5)$$

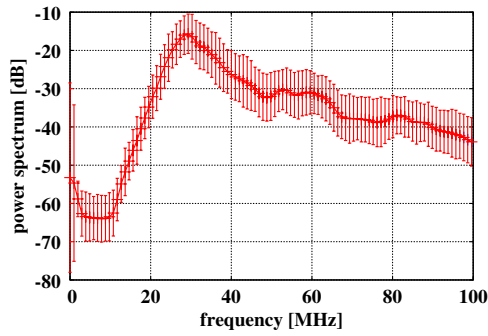


Fig. 4. (Color online) Means and standard deviations of power spectra of the ultrasound echoes reflected from the silicone plate.

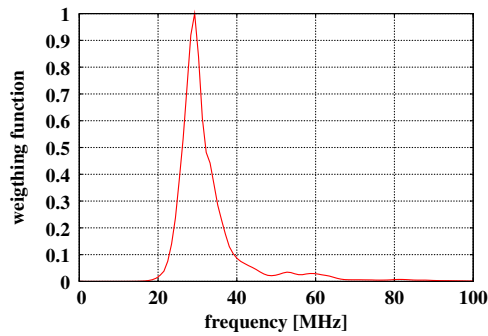


Fig. 5. (Color online) Weighting function obtained from averaged power spectrum of the ultrasound echoes reflected from the silicone plate.

where $y(f_i)$ is the normalized logarithmic power spectrum $\log_{10} P_s(f_i)/P_r(f_i)$ at an angular frequency of f_i , x_i is the logarithmic frequency $\log f_i$, and w_i is the weighting function. In this study, the weighting function w_i was defined by

$$w_i = \frac{P_r(f_i)}{P_{\text{rmax}}}, \quad (2.6)$$

where P_{rmax} is the maximum value of the power spectrum $P_r(f_i)$ from a silicone plate.

Figure 5 shows the weighting function w_i . It is assumed that the echoes due to reflection do not show frequency dependence and that only the scattering property of a target remains in the normalized power spectrum $P_s(f)/P_r(f)$.

In Rayleigh scattering, the normalized power spectrum $P_s(f)/P_r(f)$ changes linearly with respect to the logarithmic frequency. In non-Rayleigh scattering, on the other hand, the spectral slope decreases with an increase in scatterer diameter, such an increase being equal to that in the correlation length σ of the Gaussian correlation function. In this study, the diameter of the scatterer was estimated to assess RBC aggregation from the spectral slope by assuming that the correlation length σ of the Gaussian correlation function of continuous inhomogeneous media corresponds to the diameter of the scatterer.

3. Basic Experimental Results Obtained Using Microspheres

The ultrasound diagnostic equipment (Tomey UD-1000) employed is equipped with a mechanical scan probe at a center frequency f_0 of 40 MHz (wavelength is about 40 μm).

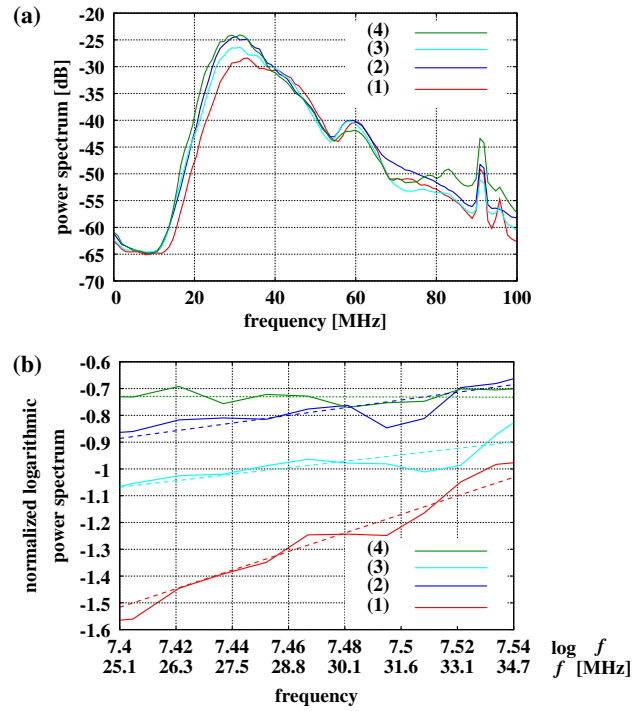


Fig. 6. (Color online) (a) Averaged power spectra of the ultrasonic echoes scattered from microspheres of various sizes and (b) normalized power spectra and the weighted least-mean-squared regression lines of microspheres (1)–(4) in Table I.

RF echoes were acquired at a sampling frequency of 1 GHz at a 16-bit resolution by the oscilloscope (Tektronix DPO7054), and their power spectra $\{P(f)\}$ were obtained by Fourier transform with a Hanning window of 1.024 μs length. To reduce the effect of random noise, 1000 power spectra were averaged. The left-hand column of Table I shows the different diameters of measured microspheres. Microspheres (1) and (3) were made of copolymer with Cl_2 , and microspheres (2) and (4) were made of copolymer without Cl_2 . Microspheres with different diameters, which were mixed with water at a concentration of 3.00 g/l, simulated nonaggregated and aggregated RBCs. This concentration is lower than that of RBCs in actual blood, preventing the aggregation of microspheres. RF echoes from the spheres around the focal point were acquired from spatially different regions by mechanical linear scan as in the measurement of a silicone plate to acquire many statistically independent data points. Effects of the difference between acoustic impedances of microspheres and RBCs were not considered in the present study, although such effects should be investigated in future studies.

Figure 6(a) shows the averaged power spectra of echoes from the microspheres, and Fig. 6(b) shows the normalized power spectra. The numbers correspond to the microsphere numbers in Table I. The spectral slope and intercept values are shown in the right-hand column of Table I. Figure 7 shows the mean and standard deviation of spectral slopes for ten measurements of each microsphere. In Fig. 5, the slope of the normalized power spectrum $P_s(f)/P_r(f)$ of a larger scatterer is smaller than that of a smaller scatterer. This result shows that the slope of the normalized logarithmic power spectrum $\log_{10} P_s(f)/P_r(f)$ is related to the diameter of the scatterer.

Table I. Microsphere diameters and experimental results.

	Particle diameter (μm)	Slope ($1/\log_{10} f$)	Intercept (dimensionless)
(1)	5 ± 2	3.46	-27.2
(2)	11 ± 3	1.78	-14.8
(3)	15 ± 5	1.47	-12.9
(4)	30 ± 10	0.02	-0.56

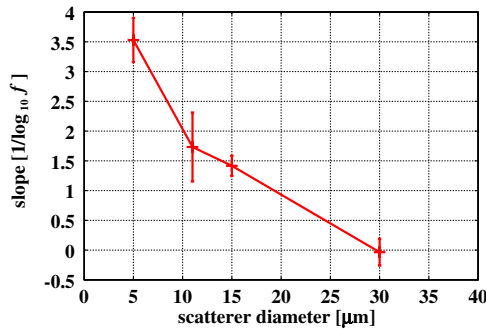


Fig. 7. (Color online) Mean and the standard deviation of the estimated spectral slopes as a function of scatterer diameter.

4. *In vivo* Experimental Results

The main components of normal blood are RBCs, which do not aggregate in large veins because of blood flow.^{21,22)} To measure ultrasonic echoes from aggregated RBCs in addition to those from nonaggregated RBCs, blood flow was stopped by pressurizing a cuff surrounding the upper arm at 250 mmHg. Ultrasonic echoes were acquired at rest for 2 min, during avascularization for 5 min, and after recirculation for 3 min. Figure 8 shows B-mode images of a vein at the dorsum manus of a 24-year-old healthy male. B-mode images were measured at rest (1), at the beginning of avascularization (2), at the end of avascularization (3), at the beginning of recirculation (4), and 120 s after recirculation (5). It is possible to reduce the attenuation of high-frequency ultrasound because the vein at the dorsum manus is a superficial blood vessel. The vein measured in this study had a large diameter and a high steady blood flow rate, which affect RBC aggregation, and thus, the measurement could be assumed to be performed with respect to the nonaggregated RBCs at rest. In addition, we measured the change in spectral slope caused by the change in blood flow rate due to avascularization using a cuff. RF echoes from the focal point positioned in the vessel lumen were acquired from many different positions by mechanical linear scan to reduce the effect of the increase in scatterer diameter variation due to aggregation.

Figure 9 shows the averaged power spectrum $P_s(f)$ of echoes from the lumen of the vein at the dorsum manus of the 24-year-old healthy male with the standard deviations. Figure 10 shows the normalized logarithmic power spectrum $\log_{10} P_s(f)/P_r(f)$ and the weighted least-mean-squared regression line. Figure 11 shows the transient change in estimated spectral slope due to avascularization. The slope of the normalized power spectrum of echoes from RBCs at rest was close to that of microsphere (3) (diameter: 15 μm) in

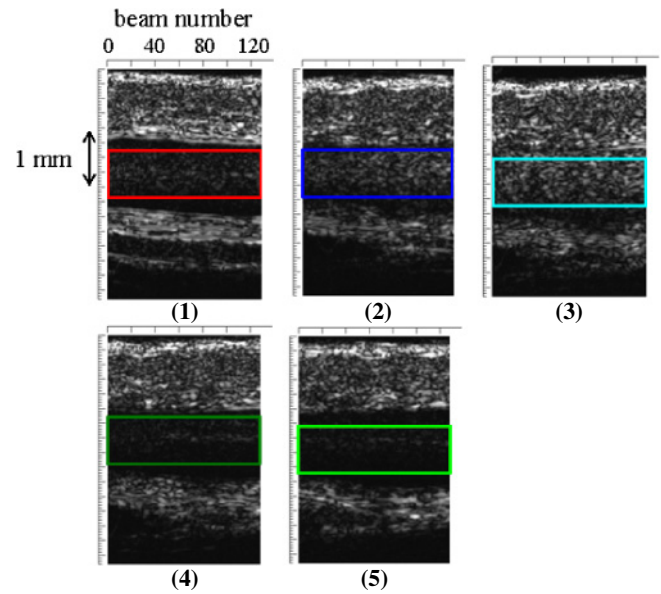


Fig. 8. (Color online) B-mode images and windows of the vein at the dorsum manus: (1) at rest, (2) at the beginning of avascularization, (3) at the end of avascularization, (4) at the beginning of recirculation, and (5) 120 s after recirculation.

Table I. The RBC diameter is 8 μm at most and this diameter is between those of microspheres (1) (diameter: 5 μm) and (2) (diameter: 11 μm). The spectral slope measured for RBCs was slightly greater than that of a sphere whose diameter corresponds to that of an RBC. One of the reasons for this was considered to be the frequency dependent attenuation of ultrasound during propagation in biological tissues. If the attenuation coefficient and the depth to vein are assumed to be 1 $\text{dB}\cdot\text{MHz}^{-1}\cdot\text{cm}^{-1}$ and 1 mm, respectively, the differences between two logarithmic normalized power spectra $\log_{10} P_s(f)/P_r(f)$ with and without attenuation are 5 dB at 25 MHz and 7 dB at 35 MHz. Accordingly, the spectral slope decreases by 1.37 in the frequency band of 25–35 MHz. Therefore, the measured spectral slope of RBCs was shown to be decreased.

Furthermore, the spectral slope gradually decreased during avascularization and returned to the levels of rest in the *in vivo* measurement. Although there are still many factors to be investigated, such as acoustic impedances of microspheres, methods for normalization, and calibration of the system,²²⁾ these results showed that the slope of the normalized power spectrum changes with scatterer diameter.

5. Conclusions

From basic experiments using microspheres, it was found that an increase in scatterer diameter led to a decrease in the slope of the normalized power spectrum. Components of Rayleigh scattering in echoes were dominant when the scatterer diameter was small. However, the larger the scatterer diameter was, the more dominant the components of the reflection were. Components of reflection showed no frequency dependence and, therefore, the spectral slope decreased.

In an *in vivo* measurement, the estimated diameter of RBCs was observed to be slightly larger than that of

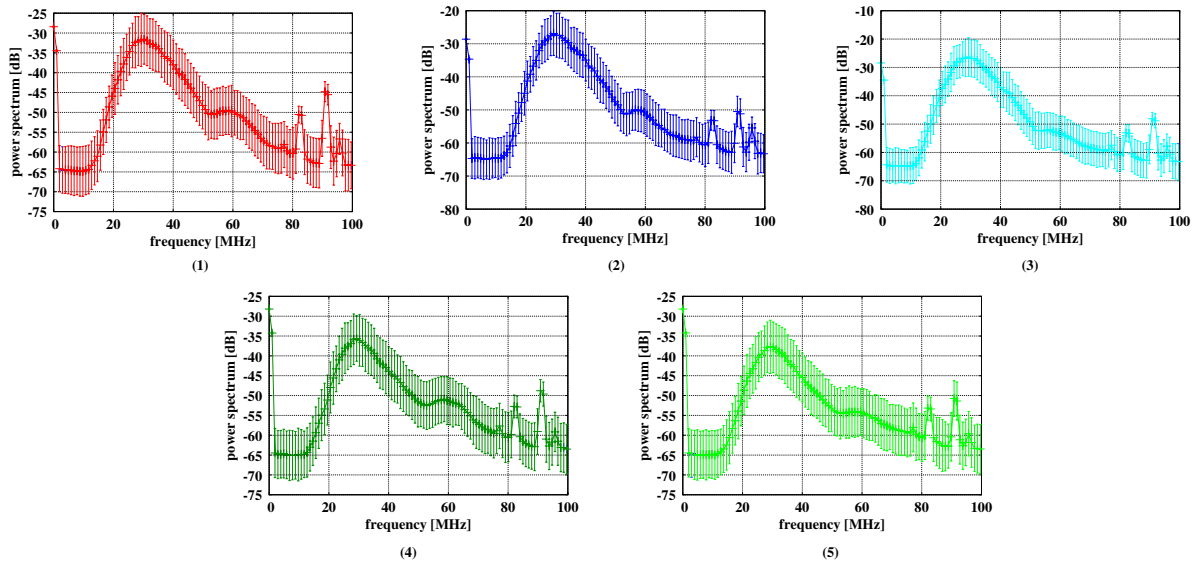


Fig. 9. (Color online) Means and standard deviations of power spectra of the ultrasonic echoes obtained for the lumen of the vein at the dorsum manus: (1) at rest, (2) at the beginning of avascularization, (3) at the end of avascularization, (4) at the beginning of recirculation, and (5) 120s after recirculation.

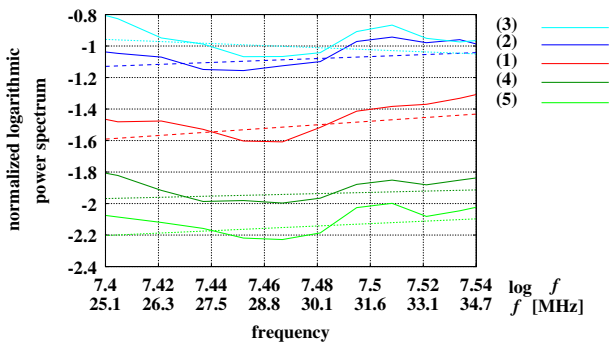


Fig. 10. (Color online) Normalized power spectra and the least-mean-squared regression lines.

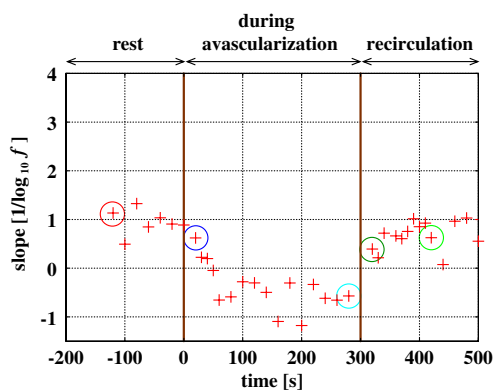


Fig. 11. (Color online) Transient change in the estimated spectral slope during avascularization for 5 min.

theoretical RBCs. This may have been caused by the frequency-dependent attenuation of ultrasound, which affected the slope. Although the estimated RBC diameter did not exactly match the real RBC diameter, these results show the possibility of utilizing the normalized power spectrum for the assessment of RBC aggregation.

Acknowledgment

We would like to thank Tomey Corporation for its cooperation on the use of the diagnostic equipment.

- 1) K. Tuzuki, H. Hasegawa, and H. Kanai: *Jpn. J. Appl. Phys.* **47** (2008) 4180.
- 2) K. Ikeshita, H. Hasegawa, and H. Kanai: *Jpn. J. Appl. Phys.* **47** (2008) 4165.
- 3) K. Ujiie: *Chinmoku no Kessen* (Silent Clots: Life's Biggest Killers) (Chuo Art Publishing, Tokyo, 2000) [in Japanese].
- 4) A. J. Vander, J. H. Sherman, and D. S. Luciano: *Human Physiology: the Mechanisms of Body Function* (McGraw-Hill, New York, 1998) p. 256.
- 5) D. G. Paeng, R. Y. Chiao, and K. K. Shung: *Ultrasound Med. Biol.* **30** (2004) 815.
- 6) A. Amararenea, J. L. Gennisson, A. Rabhi, and G. Cloutier: *IEEE Ultrasonics Symp.*, 2005, p. 874.
- 7) E. Alt, S. Banyai, M. Banyai, and R. Koppensteinerr: *Thrombosis Res.* **107** (2002) 101.
- 8) A. J. Lee, P. I. Mowbray, G. D. O. Lowe, A. Rumley, F. G. R. Fowkes, and P. L. Allan: *Circulation* **97** (1998) 1467.
- 9) C. C. Huang and S. H. Wang: *Jpn. J. Appl. Phys.* **45** (2006) 7191.
- 10) Y. Kikuchi, K. Sato, and Y. Mizuguchi: *Microvasc. Res.* **47** (1994) 126.
- 11) M. Ueda and Y. Ozawa: *J. Acoust. Soc. Am.* **77** (1985) 38.
- 12) S. Yagi and K. Nakayama: *Nihon Onkyo Gakkaishi* **36** (1980) 496 [in Japanese].
- 13) M. F. Insana, R. F. Wagner, D. G. Brown, and T. J. Hall: *J. Acoust. Soc. Am.* **87** (1990) 179.
- 14) F. T. H. Yua and G. Cloutier: *J. Acoust. Soc. Am.* **122** (2007) 645.
- 15) I. Fontaine and G. Cloutier: *J. Acoust. Soc. Am.* **113** (2003) 2893.
- 16) F. L. Lizzi, M. Greenebaum, E. J. Feleppa, M. Elbaurn, and D. J. Coleman: *J. Acoust. Soc. Am.* **73** (1983) 1366.
- 17) E. J. Feleppa, F. L. Lizzi, D. J. Coleman, and M. M. Yaremko: *Ultrasound Med. Biol.* **12** (1986) 623.
- 18) F. L. Lizzi, M. Astor, A. Kalisz, T. Liu, D. J. Coleman, R. Silverman, R. Ursea, and M. Rondeau: *IEEE Ultrasonics Symp.*, 1996, p. 1155.
- 19) K. Yamaguchi and P. K. Choi: *Jpn. J. Appl. Phys.* **45** (2006) 4621.
- 20) H. Kanai: *Oto-Shindo no Supekutoru Kaiseki* (Spectrum Analysis of Sound and Vibration) (Corona Publishing, Tokyo, 1999) [in Japanese].
- 21) S. Yagi and K. Nakayama: *Nihon Onkyo Gakkaishi* **39** (1983) 659 [in Japanese].
- 22) S. Yagi and K. Nakayama: *Nihon Onkyo Gakkaishi* **43** (1987) 777 [in Japanese].